

7th Austrian Stable Isotope User Group Meeting

Graz, November 24-25th, 2006

Hosted by:

- Karl-Franzens University, Institute of Earth Sciences, Geology and Paleontology
- Technical University Graz, Institute of Applied Geosciences, - Applied Mineralogy
- Joanneum Research, Graz, Institute for Water Resource Management

Zitiervorschlag dieses Bandes:

Bojar, A.-V., Dietzel, M., Fritz, H., Leis, A., (Hrsg.): 7th Austrian Stable isotope user group meeting.- Ber. Inst. Erdwissenschaften, K.-F.-Univ. Graz, Band 11, 50 S., Graz, 2006.

<ISSN 1608-8166>

Herausgeber und Verleger: Institut für Erdwissenschaften, Karl-Franzens-Universität Graz, Heinrichstrasse 26, A-8010 Graz, Österreich

Redaktion, Satz und Layout:

Ana-Voica Bojar¹, Martin Dietzel², Harald Fritz¹, Albrecht Leis³

¹Institut für Geologie und Paläontologie, Heinrichstrasse 26, A-8010 Graz.

²Institut für Angewandte Mineralogie, Rechbauerstraße 12

A-8010 Graz

³Institut für Wasser Ressourcen Management, Joanneum Research, Elisabethstrasse 16, A-8010 Graz.

Druckerei: Offsetdruckerei der Karl-Franzens-Universität Graz

Environmental signals in palaeosols: mineralogical and stable isotope evidence

Ana-Voica Bojar¹, Franz Ottner², Dan Grigorescu³, Hans-Peter Bojar⁴

¹Institute of Earth Sciences, Geology and Paleontology, Karl-Franzens University, Heinrichstrasse 26, A-8010 Graz, Austria, e-mail: ana-voica.bojar@uni-graz.at

²Institute of Applied Geology, Peter Jordan Strasse 70, A-1190 Wien, Austria

³Department of Geology and Geophysics, Bucharest University, Bd. Bălcescu 1, Romania

⁴Landesmuseum Joanneum, Department of Mineralogy, Raubergasse 10, A-8010 Graz, Austria

The south-western South Carpathians represent a nappe pile which is mainly composed of pre-Alpine basement nappes separated by the ophiolitic Severin unit. Within the Hațeg basin the late Cretaceous was divided by Stilla (1985) into sedimentary groups, separated by local unconformities. From Maastrichtian to Early Paleogene two different continental formations are known: the Densuș-Ciula and the Sânpetru formations both represented by continental deposit. The late Cretaceous basin subsidence correlates with the stacking of the Getic nappe on the top of the Danubian realm, as well as uplift of the surrounding areas and orogenic collapse (Bojar et al., 1998; Willingshofer et al., 2001). Burial of the Maastrichtian strata by younger deposits was limited to a few hundred meters.

At Tustea quarry, situated at the northern border of the basin, the 10 m vertical escarpment comprises two levels of massive red mudstones intercalated with conglomerates and cross-stratified sandstones. The bottom of the sequence is represented by a massive red mudstone followed by 4 m coarse grained, poorly sorted deposits with trough-cross to parallel stratification. The channel bodies show laterally crosscutting and alternating sandstones and conglomerates, which indicate unstable channelized flow with discharge fluctuations. The inter-channel areas, starved of coarse sediment supply, were site of pedogenesis. The soils show: a red mud horizon with blocky structure characterised by the presence of well developed vertical roots and burrows and a level with calcareous concretions. There are several levels of calcretes with thickness and lateral continuity indicating moderately developed soils (Retalak, 2001). Paleosols can be classified as calcisols (Mack and James, 1994). Associate with some of concretion layer, just above of them, dinosaurs nesting sites

together with embryonic/hatchling skeletal remains were found. Based on these remains, the eggs are thought to belong to a hadrosaurid *Telmatosaurus transsylvanicus* (Grigorescu et al., 1994).

X-Ray analyses show that all paleosol samples have a bulk mineralogy dominated by layer silicates. In the fraction less than 2 μm , smectite, dominates with up to 94 mass %. Other clay of minerals present in very small amounts are: illite in the range of 4 to 10 mass %, and kaolinite 2 to 4 mass %. The position of the OH band of the infrared spectrum indicate that the smectite is montmorillonite. The smectite fraction less than 0.2 μm was separated from different paleosol levels were separated in order to make additional chemical analyses and determine the isotopic composition of smectites. For isotopic composition measurements Hydrogen from the OH position and Oxygen from the OH and SiO₄ positions, absorption and interlayer water were removed by heating the samples at 200 °C for ~24 hours. Preliminary heating tests were done on STX 1 smectite standard. The samples were heated to 200°C and after each heating step an infrared spectrum and a x-ray diffraction were performed. X-ray diffraction of heated STX 1 standard shows the collapse of the (001) layer. Unheated smectite shows a (001) d-spacing of about 14.7 Å. After 5 hours at 200 °C the d-spacing is 9.74 Å. Further heating does not change the layer distance. The collapse of the layer is due to the removing of interlayer water. Infrared spectra show that only after 24 hours heating practically all interlayer water is removed, 12 hours heating was insufficient.

Stable isotope measurements on oxygen were performed using a classic silicate line with Nickel bombs. The samples were firstly heated under vacuum c. 1 day at 200°C and than fluorinated with BrF₅ at 550°C for ~ 1 day. The $\delta^{18}\text{O}$ compositions are around 19 ‰ (SMOW). For the hydrogen isotopic measurements the samples were also heated under vacuum one day at 200°C, and than measured on a TC/EA device in continuous flow. The δD values vary from -143 to -166 ‰ (SMOW). Also for the Hateg basin, measurements on the isotopic composition of the rainwater have been started in August 2006.

The calcretes show a narrow range of isotopic compositions, with $\delta^{18}\text{O}$ values between 24.1 and 25 ‰ and $\delta^{13}\text{C}$ between 8.1 and -8.9 ‰ (PDB)

At Tuştea, the red colour and the presence of calcretes with micritic texture indicate that the soils formed above the water table under oxidizing, alkaline conditions. The deeply penetrating vertical root traces also suggest well-drained soils. These conditions were favourable for the preservation of egg and bone material. The thickness and distribution of the calcrete levels indicate multiple buried, moderate to strong developed soils, most probably

developed on a stable terrace, close to the basin border. The coarse sequence is interpreted as deposited in a feeder zone of an alluvial fan during flooding events. The high content in smectite, up to 98 mass %, was favored by the presence of the volcanoclastic material present at this site. Using appropriate fractionation factors, the isotopic data indicate that the smectite are in equilibrium with the local present meteoric water line. This fact was also put in evidence by early workers (Savin and Epstein, 1970, Lawrence and Taylor, 1971). In contrast, the stable isotopic composition of calcrete are preserved reflecting the composition of paleosol water at the time of Late Cretaceous..

References:

- Bojar, A.-V., Neubauer, F., Fritz, H., 1998. Cretaceous to Cenozoic thermal evolution of the south-western South Carpathians: evidence from fission-track thermochronology. *Tectonophysics* 297, 229-249.
- Grigorescu, D., Weishampel D., Norman, D.B, Seclaman, M., Rusu, M., Baltres, A., Teodorescu, V., 1994. Late Maastrichtian dinosaur eggs from the Hațeg Basin (Romania). In: *Dinosaur eggs and babies*, Carpaner, K., Hirsch, K.F., Horner, J.R. (eds.), Cambridge University Press, 75-87.
- Lawrence, J.R., Taylor, H.P. Jr., 1971. Deuterium and oxygen-18 correlation: Clay minerals and hydroxides in Quaternary soils compared to meteoric waters. *Geochimica et Cosmochimica Acta* 35, 993-1003.
- Mack, G.H., James, C.W., 1994. Paleoclimate and the global distribution of paleosols. *Journal of Geology* 102, 360-366.
- Retallack, G.J., 2001. *Soils of the past. An introduction to paleopedology*. Blackwell Science, 404 p.
- Savin, S.M., EPSTEIN, S., 1970. The oxygen and hydrogen isotope geochemistry of clay minerals. *Geochimica and Cosmochimica Acta* 34, 35-42.
- Stilla, A., 1985. Geologie de la region de Hațeg-Cioclovina-Pui-Banita (Carpathes meridionales). -*Anuarul Institutului de Geologie si Geofizica* 66, 92-197.
- Willingshofer, E., Andriessen, P., Cloething, S., Neubauer, F., 2001. Detrital fission track thermochronology of Upper Cretaceous syn-orogenic sediments in the South Carpathians (Romania): inferences on the tectonic evolution of a collisional hinterland. *Basin Research* 13, 379-395.

Study of the sources of methane from Delta-Danube Black-Sea Region, using stable isotopes

Stela Cuna¹, Elise Pendall², John B. Miller³, Pieter P. Tans³, Ed Dlugokencky³

¹National Institute of Research and Development for Isotopic and Molecular Technologies,
Cluj-Napoca 400293, Romania

²University of Wyoming, Laramie, Wyoming 82071-3165, USA

³Earth System Research Laboratory, Global Monitoring Division, National Oceanic and
Atmospheric Administration, Boulder, Colorado 80305-3328, USA

Methane is a natural greenhouse gas, which absorbs heat and radiates it back to the surface. In fact, the methane is more potent greenhouse gas than CO₂ on a molecular basis. If we wish to slow the accumulation of CH₄ in the atmosphere to avoid the changes in climate that could result, we must understand how CH₄ is transferred from the various components of the global carbon cycle and how humans have affected the processes that control it. Major sources of methane are natural wetlands, rice agriculture, ruminant animals, natural gas emissions due to geological venting, leakage in distribution systems and coal mining, landfills and biomass burning. The Danube Delta Black Sea region of Romania is an important wetland, and this preliminary study evaluates the significance of this region as a source of atmospheric methane.

Field sampling consisted of weekly samples collected from Black Sea Constanta (BSC) site by the National Oceanic and Atmospheric Administration/ Earth System Research Laboratory (NOAA/ESRL), Global Monitoring Division, network, as well as a field trip to Danube Delta region of Romania, ca. 100 km from BSC site. In the Danube Delta area, air and water samples were collected in eight different wetland habitats by boat. CH₄ concentration in flasks and headspace above water was analyzed using a gas chromatograph with flame ionization detector. $\delta^{13}\text{C}$ for methane was analyzed by continuous flow mass spectrometry.

The methane concentrations in air and water samples from Danube Delta are high, demonstrating that Danube Delta is an important source of atmospheric methane. Water samples have highest CH₄ concentration from 1.27 $\mu\text{mol L}^{-1}$ to 9.83 $\mu\text{mol L}^{-1}$. Methane

concentration in air immediately above the wetland soil surfaces ranged from 2500 nmol mol⁻¹ to 14000 nmol mol⁻¹. These concentrations are high compared to 1800 nmol mol⁻¹ in background air (Dlugokencky et al., 1995). The $\delta^{13}\text{C}_{\text{CH}_4}$ from air samples ranged from -47 ‰ (background air) to -58 ‰ (acetate fermentation pathway) in agreement with the values reported by Breas et al. (2001).

The methane concentration in air, $[\text{CH}_4]$, and its isotopic ratio, $\delta^{13}\text{C}_{\text{CH}_4}$, may be derived from three main sources: microbially produced methane, $[\text{CH}_4]_{\text{micr}}$, fossil methane, $[\text{CH}_4]_{\text{ff}}$, and methane produced from biomass burning, $[\text{CH}_4]_{\text{bmb}}$.

$$[\text{CH}_4] = [\text{CH}_4]_{\text{micr}} + [\text{CH}_4]_{\text{ff}} + [\text{CH}_4]_{\text{bmb}} + [\text{CH}_4]_{\text{bg}} \quad (1)$$

In this equation, $[\text{CH}_4]_{\text{bg}}$ is the background for methane in air, which is defined as the smoothed marine boundary layer (MBL) at the latitude of interest (Dlugokencky et al. 1994).

We have combined the measurements of $\delta^{13}\text{C}$ with mixing ratios $[\text{CH}_4]$ in air samples to estimate the signature of the sources of methane in the Danube Delta wetland areas. We have determined these signatures with the two-end member-mixing model of Keeling. By plotting $\delta^{13}\text{C}$ vs. the inverse of the CH_4 concentration, the y-intercept is interpreted as isotopic signature of the source or sink. The isotopic signature of the methane source ranged from $\delta^{13}\text{C} = -61.1$ ‰ to $\delta^{13}\text{C} = -72.0$ ‰ suggesting the source of methane in our sampling sites in springtime was most likely to be primarily from an acetate fermentation pathway. In Fig.1 is shown a Keeling plot from one of the sampling site in Danube Delta.

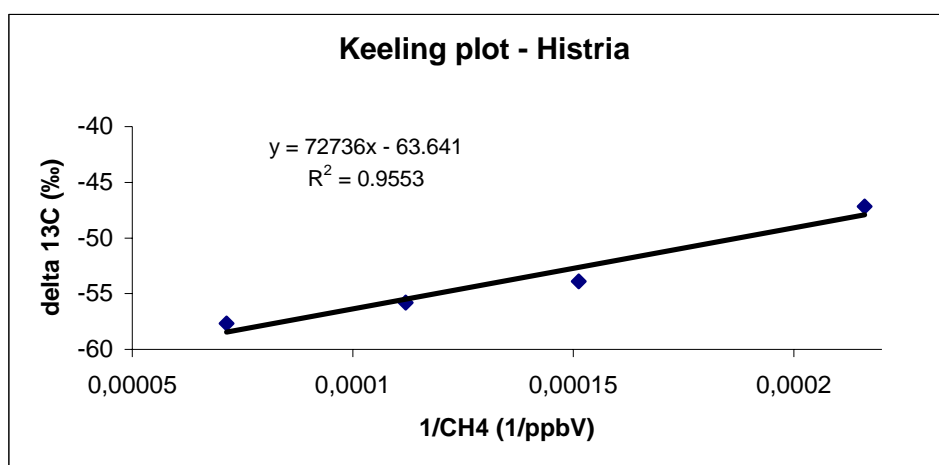


Figure 1 Keeling plot from Histria

The NOAA/ESRL CH₄ measurements from well mixed air samples were used to make the first cut of biogenic methane at the Black Sea sampling station at Constanta.

The most noticeable aspect of the BSC data is that the methane concentrations average 100-150 μmol mol⁻¹ higher than the MBL. We analyzed these data to extract the contribution of biogenic sources from global methane emissions. We assume the main influences on the mixing ratios of methane samples from BSC are biogenic, [CH₄]_{bio}, and anthropogenic (pollution), [CH₄]_{ff}. Thus, the CH₄ mole fraction is the sum of contributions from some regional background and regional fluctuations due to biogenic source and sinks and fossil fuel emissions. We can estimate [CH₄]_{bio} by taking advantage of CO measurements made on the same air used to determine [CH₄] (Miller et al., 2003). We assume that the main source of CO is pollution, mainly fossil fuel, and that there is a constant molar emission ratio of CH₄ to CO of R=0.6 for fossil fuel pollution. We estimated the methane concentrations that resulted only from biogenic and background (MBL) sources by subtracting the fossil fuel source:

$$[CH_4]_{bio,t} = [CH_4]_{BSC,t} - \Delta CO_{BSC,t} R \quad (2)$$

Figure 2 shows the estimated [CH₄]_{bio,t} from BSC corrected according to Eq. 2, with the MBL curve for comparison. We note that the corrected [CH₄] data averages roughly 100 ppb higher than the MBL curve, showing a consistent and significant biological source. We concluded that the most of the methane at the BSC station is not from pollution.

Preliminary Keeling plots from the BSC air flask samples show a lower δ¹³C source value in summer (-55‰), similar to the microbial methanogenesis value, and a higher value in winter (-51‰). These isotope data are consistent with the possibility of greater biological contributions to elevated CH₄ concentrations in summertime, and greater anthropogenic contributions to elevated concentrations in winter at the Black Sea – Constanta sampling station.

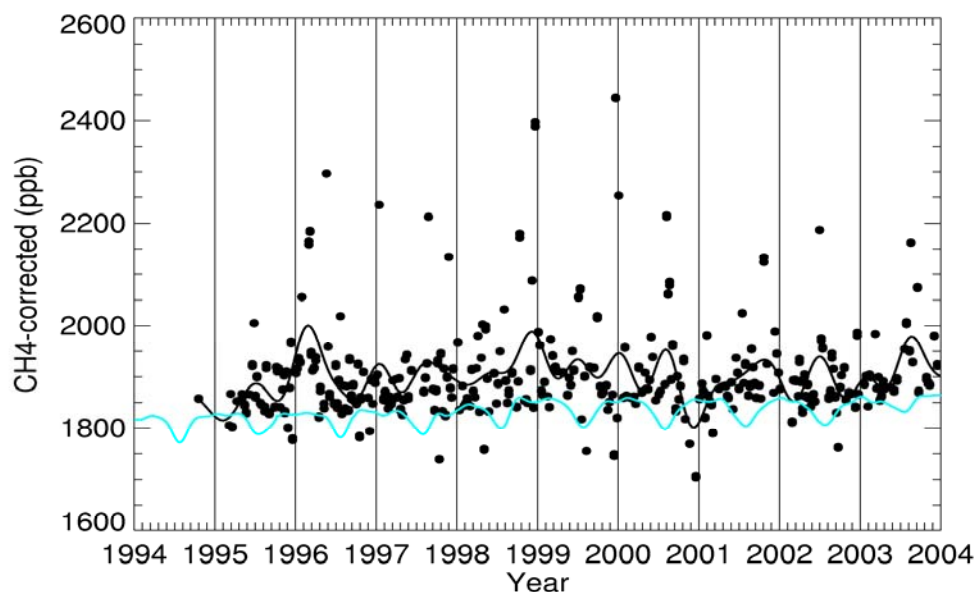


Figure 2. Time series of $[\text{CH}_4]$ from BSC corrected to remove the fossil fuel source. Black line, smoothed curve fit to the corrected CH_4 data; grey line, MBL reference.

The Delta Danube is a biological source of methane, but the samples collected at BSC have biogenic, fossil fuel and geological methane contributions.

References

Breas, O., Guillou, C., Reniero, F., Wanda, E., 2001. Review of the global methane cycle: isotopes and mixing ratios, sources and sinks. *Isotopes Environ. Health Stud.* 37, 257-378.

Dlugokencky, E.J., Steele, L.P., Lang, P.M., Masarie, K.A., 1995. Atmospheric methane at Mauna Loa and Barrow observatories: Presentation and analysis of in situ measurements. *J. Geophys. Res.* 100(D11), 23,103-23,113, doi: 10.1029/95JD0246

Dlugokencky, E.J., Steele, L.P., Lang, P.M., Masarie, K.A., 1994. The Growth-Rate and Distribution of Atmospheric Methane. *Jeophys. Res.* 99(D8), 17021-17043

Miller, J.B., Tans, P.P., White, J.W.C., Conway, T.J., Vaghan, B.W., 2003. The atmospheric signal of terrestrial carbon isotopic discrimination, and its implication for partitioning carbon fluxes. *Tellus* 55B, 197-206.

Study of the authenticity and regional origin of Romanian wines using Isotope Ratio Mass Spectrometry

Stela Cuna, Nicolae Palibroda, Gabriela Balas

National Institute for Research and Development of Isotopic and Molecular
Technologies, Donath Str. 71-103, Cluj Napoca 400293, Romania

The measurement of natural abundance of isotopes has been mainly used in geochemistry and environmental research. Since a few years the isotopic techniques have also gained a growing interest for the control of food products and beverages. This paper presents the development of an analytic technique for the determination of isotope ratios as a tool for authenticity proof of wines.

Two analytical techniques are mainly used for the measurements of the stable isotope content in wines. These are the Isotope Ratio Mass Spectrometry (IRMS) for $^{13}\text{C}/^{12}\text{C}$, $^{18}\text{O}/^{16}\text{O}$, $^2\text{H}/^1\text{H}$ and the deuterium Nuclear Magnetic Resonance (^2H -NMR).

Wine has been one of the products analysed either for improvement of quality or for detection of possible frauds. Wine is obtained by fermentation of grape must and its alcohol grade is proportional to the initial sugar concentration of the must. An increase of the alcohol grade of wine can be obtained by addition of foreign sugars before or during fermentation. In the European Union this practice, called chaptalisation, must be in compliance with the European Regulation that stipulates maximum levels of enrichment for the various European wine growing areas. The chaptalisation with cane sugar is easily detectable by IRMS because of significant increase of the ^{13}C content of the ethanol resulting from the fermentation of the mixture of C_4 cane and C_3 grape sugar. On the other hand, because of the same C_3 metabolism of grape and beet, the chaptalisation with beet sugar can be detected by using quantitative deuterium NMR.

The content of ^{18}O in water from wine is performed by IRMS and is used for the detection of addition of water, for the characterisation of the geographical origin of wines and for the establishment of the year of vintage. The European Community has adopted the determination of ^{18}O from wine as an official method for analysis of wines and has included this parameter in the E.U. Wine Databank.

The $^{13}\text{C}/^{12}\text{C}$ –IRMS method is used for the detection of the geographical origin of

wine, year of vintage, mixture of C₃ and C₄ sugars in wine, and for detection of addition of glycerol. This method is used for the characterisation of natural gasification of sparkling wines, too.

The method enables measurements of the ¹³C/¹²C isotope ratio in wine ethanol. The information on ¹³C content enables the quantities of mixtures of sugar or alcohol derived from C₃ and C₄ plants to be determined.

The ¹³C/¹²C content is determined on carbon dioxide produced during the complete combustion of the ethanol. The ethanol must be extracted from the wine before isotopic analysis. This is carried out by distillation of wine.

The apparatus for extracting ethanol comprises an electric heating mantle with voltage regulator, one litre round-bottom flask with ground glass neck joint, a column filled with Dixon metallic rings, a flask for collecting the ethanol, and a distilling controller automatic controlled.

The ethanol is quantitatively converted into carbon dioxide in sealed glass bulb filled with copper oxide as an oxidation agent. The carbon dioxide is purified of all other combustion products including water.

All the process has to be without any isotopic fractionation. All steps of the preparation must be carried out without any significant ethanol loss through evaporation that would change the isotopic composition of the sample.

The isotopic analysis was performed with a mass spectrometer capable of determining the relative ¹³C content of naturally occurring gas with an internal accuracy of 0,3‰ or better expressed as a relative value.

The ionic current for m/z=45 is corrected for the contribution of ¹²C¹⁷O¹⁶O which is calculated according to the current intensity measured for m/z=46, while taking the relative abundance of ¹⁸O and ¹⁸O into account (Craig correction). Comparison with a reference calibrated against the international reference V-PDB permits calculation of carbon content on the δ¹³C relative scale.

It was distilled 500ml wine to verify the parameters of the distillation column and the recoverable quantity of the ethanol from wine.

We found that a good reflux ratio (the ratio of the reflux to the distillate) was 20. The time needed for the distillation of the wine sample was about 4 hours. In this time it has collected three fractions from distillate:

- fraction I at 35 min, about 5ml distillate

- fraction II at 185 min, about 75ml distillate
- fraction III at 230 min, about 5ml distillate.

Every fraction was analyzed by gas chromatography to see its composition. The composition of the fraction I and II was carried out with a FID detector. The composition of fraction II and III was carried out with a thermal conductivity detector. The fraction I contained some impurities that are more volatile than ethanol (aldehydes and esters). The fraction II contained ethanol with very low level of impurities. The content of water from this fraction (6%) is normally because the ethanol is an azeotrop mixture with water in proportion of 95.6% ethanol and 4.4% water. The fraction II is good for isotopic analysis and we have used it for measuring $\delta^{13}\text{C}$ in ethanol.

The fraction III has a high content of water and low content of ethanol. The residuum of distillation contains water as major component and can be used to analyse ^{18}O in water from wine.

The samples of wine from the 2002 vintage and from six different wine-growing regions of Romania were analyzed.

The composition of ^{13}C , ^{18}O and D from 25 wine samples was established by analysis with a commercially modernized mass spectrometer respectively with a home made deuterium analysis mass spectrometer SMAD-1.

The results were presented in Table 1 and 2.

Table 1. The isotopic composition of the ^{13}C , ^{18}O and D from 11 white wine samples

Sample	Type of wine	$\delta^{18}\text{O}_{\text{SMOW}}$ (‰)		$\delta^{13}\text{C}_{\text{PDB}}$ (‰)	$\delta\text{D}_{\text{SMOW}}$ (‰)
		wine	reziduu		
1.	Feteasca Alba, Tohani 2002	-0.57	+6.27	-25.75	23.8
2.	Feteasca Alba, Bucium 2002, final	-0.34	+3.12	-25.75	9.13
3.	Feteasca Alba, Cotnari 2002, start	+0.70	+1.89	-25.86	10.02
4.	Feteasca Alba, Cotesti 2002		+2.94	-25.16	16.56
5.	Feteasca Alba, Stefanesti 2002, final	+1.26	+2.51	-25.13	12.58

6.	Feteasca Alba, Aiud 2002, start	-2.60	+3.03	-25.61	26.24
7.	Feteasca Alba, Tohani 2002, final	+0.52	+7.34	-25.15	31.3
8.	Feteasca Alba, Bucium 2002, final	-3.58	+7.07	-26.84	26.76
9.	Feteasca Alba, Cotnari 2002, final	-0.61	-0.94	-26.05	7.64
10.	Feteasca Alba, Cotesti 2002	+3.28	+10.23	-26.22	48.02
11.	Feteasca Alba, Stefanesti 2002, Final	-0.68	+5.32	-25.61	41.13

Table 2. The isotopic composition of the ^{13}C , ^{18}O from 14 wine samples

Sample	Type of wine	$\delta^{18}\text{O}_{\text{SMOW}}$ (‰)	$\delta^{13}\text{C}_{\text{PDB}}$ (‰)
1.	Cabernet Sauvignon, Tg. Bujor, 2004, red wine	0.10	-26.74
2.	Cabernet Sauvignon, Murfatlar, 2004, red wine	0.23	-28.41
3.	Cabernet Sauvignon, Tohani, 2003, red wine	5.35	-24.67
4.	Cabernet Sauvignon, V. Calugareasca, 2004, red wine	-0.18	-27.48
5.	Cabernet Sauvignon, V. Calugareasca, 2003, red wine	4.16	-24.86
6.	Cabernet Sauvignon, Tohani, 2004, red wine	1.89	-27.05
7.	Cabernet Sauvignon, Murfatlar, 2003, red wine	1.13	-26.98
8.	Cabernet Sauvignon, Bujoru, 2003, red wine	3.40	-24.57
9.	Feteasca Regala, Copou, 2002, white wine	-5.87	-29.00
10.	Feteasca Regala, Aiud, 2002, white wine, final	-1.60	-25.56
11.	Feteasca Regala, Dragasani, 2002, white wine, start	-3.46	-28.18

12.	Feteasca Regala, Copou, 2004, white wine	-0.52	-26.22
13.	Feteasca Regala, Aiud, 2004, white wine	-1.15	-25.93
14.	Feteasca Regala, Dragasani, 2004, white wine	0.80	-27.89

In this study we have developed a method for measuring $^{13}\text{C}/^{12}\text{C}$ and $^{18}\text{O}/^{19}\text{O}$ in wine ethanol and water from wine and we have studied the possibility to extract the ethanol from wine by distillation, without isotopic fractionation. The most propitious parameter of the distillation column was determined. Also we have determined the composition of ^{13}C , ^{18}O and D from some wine samples from different regions of Romania. These methods will be further used for the constitution of a databank of isotope ratios of wine.

$^{13}\text{C}/^{12}\text{C}$ and $^{18}\text{O}/^{16}\text{O}$ Signatures of calcite sinter in alkaline drainage solutions – Proxy for precipitation mechanisms

Martin Dietzel¹, Thomas Rinder¹, Albrecht Leis², Stephan Köhler¹, Dietmar Klammer¹, Peter Reichl²

¹Institute of Applied Geosciences, Graz University of Technology, Austria

email: martin-dietzel@tugraz.at

²Institute of Water Resources Management, Joanneum Research Graz, Austria

³Institute of Earth Science, University of Graz, Austria

Drainage systems of tunnels are often a target of scale sintering. In general, such sinter material mainly consists of calcite. Calcite sinter in drainage systems may induce serious problems due to the reduction of cross sections of drainage tubes and the pollution of receiving streams by suspended calcite and ongoing sinter formation.

The aim of the present study is to decipher the mechanisms and kinetics of calcite sinter formation by analyzing the chemical and isotopic composition, $^{13}\text{C}/^{12}\text{C}$ and $^{18}\text{O}/^{16}\text{O}$ ratios, of the drainage solutions and precipitated calcite. Fundamental knowledge about the dynamics and element cycles within such systems are required to develop suitable retaliatory action.

In general, the precipitates consist of about 90 to 95 wt.% calcite with minor amounts of magnesium as well as traces of silica, iron, and aluminium (e.g. detritical silicates like clay minerals, and quartz). The drainage solutions typically exhibit elevated pH values vs. those of the groundwater. The pH can even reach values between 12.3 and 13.2. Such high alkaline drainage solutions are generated from groundwater by strong interaction with the shotcrete of the tunnel construction, whereas less slightly alkaline solutions are due to rather reduced solid-liquid interaction or mixtures of various solutions. Reaction mechanisms at the shotcrete can be followed by high alkaline drainage solution vs. groundwater composition. E.g. depletion of dissolved magnesium and sulfate indicates the formation of ettringite (or thaumasite and gypsum) and brucite ($\text{Mg}(\text{OH})_2$). However, the formation of the alkaline environments is mostly related to the dissolution of portlandite ($\text{Ca}(\text{OH})_2$) from concrete.

In general, calcite-sinter is related to the dissolved inorganic carbon of ground waters. Nevertheless, great quantities of sinter may also occur in tunnels where ground waters are low

in dissolved carbonate (e.g. in areas dominated by sandstone or shale). Moreover, precipitation of calcite continues also in those ground waters generated in carbonate rich areas, although the primary dissolved carbonate is already lost. This may suggest an influence of atmospheric CO₂. Gaseous carbon dioxide is absorbed into the solution and thus contributes to further precipitation of calcite.

The results show that both mechanisms, precipitation of carbonate from ground water and absorption of atmospheric CO₂, may be deciphered by the stable isotopic composition of carbon and oxygen in the precipitated calcite. In general, solid CaCO₃ obtained by atmospheric CO₂-absorption has a δ¹³C-value of about -25 ‰ (PDB), whereas precipitation of CaCO₃ from ground water carbonate implies the characteristic isotopic signature δ¹³C ≈ -13 ‰ (PDB).

The fixation of atmospheric ¹²CO₂ and ¹³CO₂ in the precipitated calcite is accompanied with a kinetic fractionation. Diffusion and hydroxylation of ¹³CO₂ is slower vs. ¹²CO₂. In this situation, the isotopic composition of the calcite-sinter is obtained by equation

$$\delta^{13}\text{C}_{\text{CaCO}_3(2)} + 10^3 = \alpha \cdot \beta^{0.5} \cdot (\delta^{13}\text{C}_{\text{CO}_2(\text{atm})} + 10^3) \quad (1)$$

where α and β denote the equilibrium fractionation coefficient between dissolved and solid carbonate (α = 1.0011) and the kinetic fractionation coefficient via diffusion and hydroxylation of CO₂ (β = 0.9614). Thus, isotopic fractionation between precipitated calcite and gaseous CO₂ is (α · β^{0.5} - 1) · 10³ = -18.4 ‰. Considering δ¹³C_{CO₂(atm)}} = -7 ‰ of the atmosphere an isotopic composition of calcite-sinter of about -25.4 ‰ is obtained.

For δ¹³C-values higher than -25 ‰ CO₂-absorption may be superimposed by dissolved bicarbonate derived from ground waters. Values down to -29 ‰ are related to CO₂-absorption from a mixture of atmospheric CO₂ and CO₂ from combustion of fossil fuel with “light” isotopic values. For example, calcite-sinter with δ¹³C ≈ -29 ‰ implies gaseous CO₂ of about -11 ‰.

In general, solid CaCO₃ obtained by atmospheric CO₂-absorption has a δ¹³C- and δ¹⁸O-value of about -25 and -20 ‰ (PDB), respectively, whereas precipitation of CaCO₃ from groundwater carbonate implies a characteristic isotopic signature δ¹³C ≈ -13 ‰ and δ¹⁸O ≈ -5 ‰ (PDB). The type and relative amount can be evaluated by the stable isotopic composition of carbon and oxygen in the precipitated calcite (Fig.1).

Accordingly, along the flow path and exposure of the alkaline drainage solution to the atmosphere stable carbon isotope signatures of the dissolved inorganic carbon (DIC) show an increasing influence of atmospheric CO_2 . This is documented by a respective increase of $\delta^{13}\text{C}_{\text{DIC}}$ -values of the solutions.

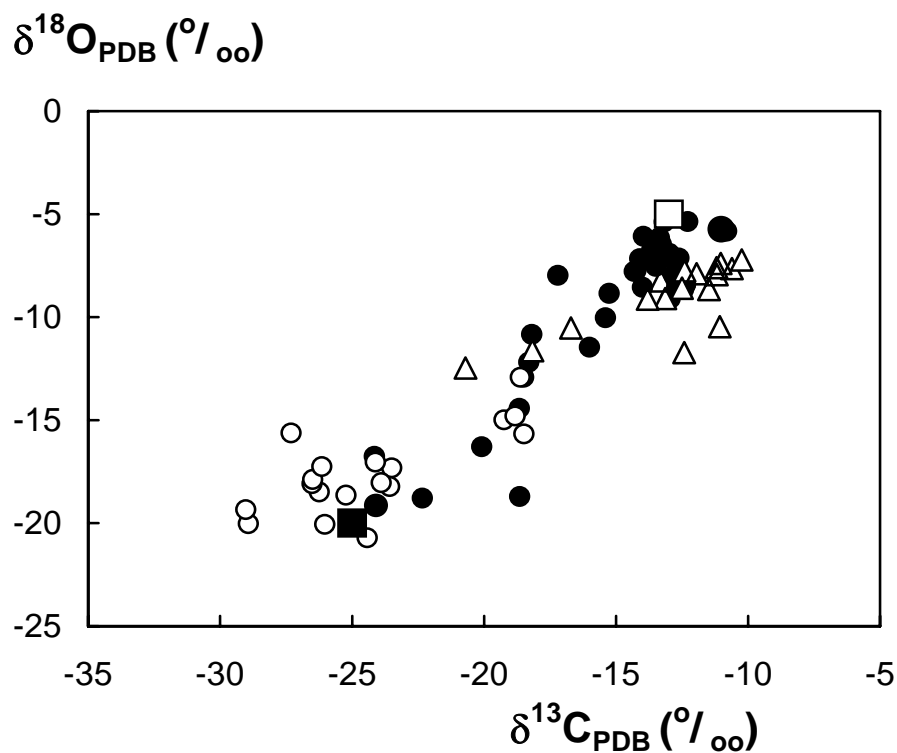


Figure 1. Distribution of $^{13}\text{C}/^{12}\text{C}$ and $^{18}\text{O}/^{16}\text{O}$ isotopes of precipitated calcite.

Δ : “Koralmerkundungsstollen (Austria)”

\bullet : “Leinebuschtunnel (Germany)”

\circ : sinter formation on concrete

\blacksquare : precipitation from CO_2 -absorption in $\text{Ca}(\text{OH})_2$ solution (experiment)

\square : precipitation from groundwater carbonate

Controls of calcium isotope fractionation in biogenic and inorganic calcium carbonate

Nikolaus Gussone^{1,2}

¹Forschungszentrum Ozeanränder der Universität Bremen, Leobener Straße,
D-28359 Bremen, Germany

²Institut für Mineralogie, Universität Münster, Corrensstr. 24, D-48149 Münster, Germany

Calcium is a widely distributed element on earth and plays an important role in many geological and biological processes. In the marine realm, Ca is of particular interest because the Ca concentration affects the evolution of life in the ocean and due to the precipitation and dissolution of CaCO₃, calcium is linked to the oceanic carbon cycle and global climate. Since Ca isotopes are considerably fractionated during biogenic CaCO₃ precipitation, the isotopic composition of skeleton elements (bones, shells, test) can be used to reconstruct past climate variability: Calcium isotopes were for instance used to reconstruct the relation of organisms in ancient food chains (Skulan et al., 1997; Clementz et al., 2003), the isotopic composition of seawater, reflecting changes of the oceanic Ca-budget cf. (De La Rocha and DePaolo, 2000; Fantle and DePaolo, 2005; Heuser et al., 2005; Schmitt et al., 2003) and paleotemperatures (Zhu and Macdougall, 1998; Nägler et al., 2000; Gussone et al., 2004; Hippler et al., 2006). One particular feature of Ca isotope fractionation is the establishment of two considerably different temperature sensitivities in different planktonic marine species, which allow the use of Ca isotopes for the reconstruction of temperatures as well as seawater isotopic composition, provided that appropriate species are selected for the respective application.

For the application of Ca isotopes as proxy and their reliable paleoclimatic interpretation it is important to understand what mechanisms influence Ca isotope fractionation and what environmental factors have to be considered. In general, the Ca isotopic composition of biogenic carbonates can be influenced by inorganic and biological fractionation processes, which are characterised by different fractionation behaviour in response to different environmental parameters.

During inorganic CaCO₃ precipitation light Ca isotopes are enriched in the solid, relative to the solution. This behaviour differs from the oxygen isotope system, incorporating preferentially the heavy isotopes in the solid. The extent of Ca isotope fractionation depends,

like in other isotope systems, on the crystal structure of the solid phase. For instance calcium isotopes in aragonite are, like in the oxygen isotope system, stronger fractionated than calcite; i.e. lighter Ca isotopes (Gussone et al., 2005) but heavier oxygen isotopes cf. (Böhm et al., 2000) are incorporated into aragonite compared to calcite. Like in the oxygen isotope system, Ca isotope fractionation decreases with increasing temperature, leading to a positive correlation between temperature and Ca isotopy, while $\delta^{18}\text{O}$ is inversely correlated to temperature. As well, the observed temperature sensitivity of oxygen and Ca isotope fractionation in inorganic CaCO_3 differs significantly. While $\delta^{18}\text{O}$ changes with a rate of about $-0.2\text{‰}/^\circ\text{C}$, the temperature dependence of Ca isotope fractionation is about $0.02\text{‰}/^\circ\text{C}$ cf. (Gussone et al., 2003; Marriott et al., 2004). While the oxygen isotope signal is caused by decreasing equilibrium fractionation with increasing temperature, the temperature dependence of Ca isotope fractionation was recently proposed to be caused by changes in precipitation rate (Lemarchand et al., 2004). In this model, Lemarchand et al. (2004) suggested that the temperature dependence found in inorganic CaCO_3 can be explained by the temperature-dependent speciation of the carbonic acid (Millero, 1995), leading to an increase in $[\text{CO}_3^{2-}]$ with increasing temperature. The increase in $[\text{CO}_3^{2-}]$ then leads to a higher saturation state of calcite/aragonite and to increasing precipitation rates, resulting in reduced Ca isotope fractionation in the calcium carbonate.

In contrast to the inorganic precipitated CaCO_3 , the calcite skeletons of some marine foraminifers (*O. universa*) and coccolithophores (*E. huxleyi*) show a similar temperature dependence, but no major response to CO_3^{2-} -changes. These results indicate a biological control of the fluid chemistry inside the vesicle, in which CaCO_3 precipitation takes place (Gussone et al., 2006).

References

- Böhm, F., Joachimski, M. M., Dullo, W. C., Eisenhauer, A., Lehnert, H., Reitner, J., Wörheide, G., 2000. Oxygen isotope fractionation in marine aragonite of coralline sponges. *Geochim. Cosmochim. Acta* 64(10), 1695-1703.
- Clementz, M. T., Golden, P., Koch, P. L., 2003. Are Calcium Isotopes a Reliable Monitor of Trophic Level in Marine Settings. *International Journal of Osteoarcheology* 13, 29-36.
- De La Rocha, C. L., DePaolo, D. J., 2000. Isotopic Evidence for Variations in the Marine Calcium Cycle Over the Cenozoic. *Science* 289, 1176-1178.

- Fantle, M. S., DePaolo, D. J., 2005. Variations in the marine Ca cycle over the past 20 million Years. *Earth and Planetary Science Letters* 237, 102-117.
- Gussone, N., Böhm, F., Eisenhauer, A., Dietzel, M., Heuser, A., Teichert, B. M. A., Reitner, J., Wörheide G., Dullo, W.-C., 2005. Calcium Isotope Fractionation in Calcite and Aragonite. *Geochimica et Cosmochimica Acta* 69(18), 4485-4494.
- Gussone, N., Eisenhauer, A., Heuser, A., Dietzel, M., Bock, B., Böhm, F., Spero, H. J., Lea D. W., Bijma, J., Nägler, T. F., .2003. Model for Kinetic Effects on Calcium Isotope Fractionation ($\delta^{44}\text{Ca}$) in Inorganic Aragonite and Cultured Planktonic Foraminifera. *Geochimica et Cosmochimica Acta* 67(7), 1375-1382.
- Gussone, N., Eisenhauer, A., Tiedemann, R., Haug, G. H., Heuser, A., Bock, B., Nägler, T. F., Müller, A., 2004. $\delta^{44}\text{Ca}$, $\delta^{18}\text{O}$ and Mg/Ca Reveal Caribbean Sea Surface Temperature and Salinity Fluctuations During the Pliocene Closure of the Central-American Gateway. *Earth and Planetary Science Letters* 227, 201-214.
- Gussone, N., Langer, G., Thoms S., Nehrke, G., Eisenhauer, A., Riebesell, U., Wefer, G., 2006. Cellular calcium pathways and isotope fractionation in *Emiliana huxleyi*. *Geology* 34(8), 625-628.
- Heuser, A., Eisenhauer, A., Böhm, F., Wallmann, K., Gussone, N., Pearson, P. N., Nägler, T. F., Dullo, W.-C., 2005. Calcium Isotope ($\delta^{44}\text{Ca}$) Variations of Neogene Planktonic Foraminifera. *Paleoceanography* 20(PA2013), doi:10.1029/2004PA001048.
- Hippler, D., Eisenhauer, A., Nägler, T. F., 2006. Tropical Atlantic SST history inferred from Ca isotope thermometry over the last 140 ka. *Geochimica et Cosmochimica Acta* 70, 90-100.
- Lemarchand, D., Wasserburg G. J., and Papanastassiou D. A., 2004. Rate-controlled Calcium Isotope Fractionation in Synthetic Calcite. *Geochim. Cosmochim. Acta* 68(22), 4665-4678.
- Marriott C. S., Henderson, G. M., Belshaw, N. S., Tudhope, A. W., 2004. Temperature dependence of $\delta^7\text{Li}$, $\delta^{44}\text{Ca}$ and Li/Ca during growth of calcium carbonate. *Earth and Planetary Science Letters* 222, 615-624.
- Nägler, T. F., Eisenhauer, A., Müller, A., Hemleben, C., Kramers, J., 2000. $\delta^{44}\text{Ca}$ - Temperature Calibration on Fossil and Cultured Globigerinoides sacculifer: New tool for reconstruction of past sea surface temperatures. *Geochemistry, Geophysics, Geosystems* 1, doi:10.1029/2000GC000091.

- Schmitt, A. D., Stille, P., Vennemann, T., 2003. Variations of the $^{44}\text{Ca}/^{40}\text{Ca}$ ratio in seawater during the past 24 million years: Evidence from $\delta^{44}\text{Ca}$ and $\delta^{18}\text{O}$ values of Miocene phosphates. *Geochimica et Cosmochimica Acta* 67(14), 2607-2614.
- Skulan, J., DePaolo, D. J., Owens, T. L., 1997. Biological control of calcium isotopic abundances in the global calcium cycle. *Geochim. Cosmochim. Acta* 61(12), 2505-2510.
- Zhu, P. Macdougall, D., 1998. Calcium isotopes in the marine environment and the oceanic calcium cycle. *Geochimica et Cosmochimica Acta* 62(10), 1691-1698.

Historical Carbonate Mortar and Plaster - Isotopic and Chemical Signatures

Barbara Kosednar-Legenstein¹, Martin Dietzel¹, Albrecht Leis², Bettina Wiegand³,
Karl Stingl¹, Miriam Baumgartner¹

¹Institute of Applied Geosciences, Graz, Austria, e-mail: Kosednar-legenstein@TUGraz.at

²Institute of Water Resources Management, Joanneum Research Graz, Austria

³Department of Geological and Environmental Sciences, Stanford University,

The main focus of this study is to investigate the mineralogical, chemical and isotopic composition of historic carbonate binders and local limestone deposits. Mortar and plaster samples of roman, medieval and pre-industrial buildings were sampled in Styria/Austria (Eisenerz, Thörl, Kleinstübing, Niederhofen, Graz, Flavia Solva, Kainach, Deutschlandsberg, Kapfenstein) as well as samples from chalk-pits, marble and dolomite quarries close to the corresponding historical buildings. In several samples the historic age gained from archaeological aspects was confirmed by ¹⁴C dating. The respective mortars and plasters mostly consist of CaCO₃ (calcite) as cement with aggregates of calcite, dolomite, quartz, and other silicates like clay minerals or mica.

The ⁸⁷Sr/⁸⁶Sr ratios of the cement are between 0.7091 and 0.7115, whereas Sr/Ca ratios do not exceed 0.003. In principle, these ratios reflect the composition of the natural deposits used for manufacturing of lime mortar. The ⁸⁷Sr/⁸⁶Sr values depend on the geologic environment and mineralogical composition of the primary limestone.

Burning and setting experiments were conducted in laboratory to investigate the behaviour of REE and the strontium isotopes. Burning has a negligible influence on Sr/Ca, ⁸⁷Sr/⁸⁶Sr ratios and REE distribution, and rather minor effects may be caused by aggregate leaching during CaCO₃ setting. However, in several cases Sr/Ca and ⁸⁷Sr/⁸⁶Sr signatures can be used as a kind of fingerprint.

The ¹³C/¹²C and ¹⁸O/¹⁶O composition of the carbonate cement comprise a wide range of $\delta^{13}\text{C}_{\text{CaCO}_3}$ (PDB) from -24 to -1‰, and of $\delta^{18}\text{O}_{\text{CaCO}_3}$ (PDB) from -24 to -3‰. The $\delta^{13}\text{C}$ and $\delta^{18}\text{O}$ distribution shows an almost linear correlation. In general, calcite is isotopically lighter at the exterior versus the interior mortar layer. The range and systematic correlation of

the data reflect isotopic fractionation effects upon setting of the cement and during the history (e.g. re-crystallization and weathering) of the cement.

The $^{13}\text{C}/^{12}\text{C}$ distribution depends on kinetic fractionation due to hydroxylation of gaseous CO_2 , resulting in an enrichment of ^{12}C versus ^{13}C in the precipitated CaCO_3 . Upon setting of the cement, the diffusion of gaseous CO_2 leads to a continuous enrichment of ^{13}C and ^{18}O of CO_2 within the gas phase along the cement setting path. This is confirmed by laboratory sequential precipitation experiments. Accordingly, precipitated calcite is isotopically heavier at the interior mortar layer. Variations may be caused by natural or anthropogenic impacts, e.g. evaporation of H_2O during the setting or CO_2 from anthropogenic origin. On the other side, CO_2 from burning of fossil fuels and soils or re-crystallization of carbonate cements in the presence of H_2O from various origins may be deciphered.

Impact of transboundary air pollution on sensitive karst water resources by means of N-, O-, Pb-, S- and Sr-isotopes

Martin Kralik¹, Franko Humer¹, Johanna Nurmi-Legat¹, Andrea Hanus-Illnar¹, Johannes Grath¹, Michael Mirtl¹, Maria-Theresia Grabner¹, Stan Halas² & Monika Jelenc³

¹Umweltbundesamt GmbH (Federal Environment Agency Ltd), Austria,
martin.kralik@umweltbundesamt.at

²Mass Spectrometry Laboratory, Marie-Curie-Sklodowska Univ. Lublin, Poland

³Geochronology Lab., Center for Earth Sciences, Univ. of Vienna, Austria

Introduction

The impact of air pollution is a substantial European and global problem which was observed even in the most remote areas of our planet. Not only surface water, but also groundwater re-sources are partly endangered by dry and wet deposition from the air. Karst and other sensitive aquifers contribute up to 90 % to the total drinking water supply in some European regions. However, they are more vulnerable to contamination than other aquifers due to short transfer times from recharge to source. Therefore, the main objective of this paper is to show possibilities to quantify the impact of air pollution on sensitive water resources (e.g. karst), to develop an innovative surveillance tool based on isotopes and meteorological considerations.

In a pilot study on a small number of samples as precipitation, soil, rock and spring waters were collected in the North front of the Northern Calcareous Alps to test the application of isotope analyses to estimate the amount of far transported contaminants and their impact on the spring water quality. The hydrochemistry and the isotopic composition of nitrate, sulphate, strontium, lead and the water molecule itself has been analysed in five laboratories, each of them specialised in a certain group of isotopes.

Investigation site

The Federal Environmental Agency Vienna runs an UN-ECE-Integrated Monitoring station (Zoebelboden) within a karstified dolomite. The Zoebelboden-site is located south of Linz (Upper Austria) in the front range of the Northern Calcareous Alps in form of steep mountain ridges at an altitude of 500-950 m. The monitoring sites are divided in plateau and

slope areas. The natural mixed mountain forest (beech, fir) is often displaced by production forest dominated by spruce. Transeuropean air masses coming mainly from NW are washed out by relatively high precipitation rates (1650 mm/year). On this Zoebelboden-site in the National Park "Nördliche Kalkalpen" a geology, hydrology and hydrogeology research program is running since 1993. Hydrogeological and hydrochemical well studied springs are accessible in winter time. Studies with fluorescence tracers showed passage times of about 20 hrs during storm events.

Materials and Method

Sampling

The precipitation was collected as monthly sample either in a wet only sampler (WADOS) installed on top of a research container with immediate cooling (4°C) or with three large containers as open deposition during May till December 2005.

The spring water samples and their suspended matter were all collected during August and December 2005 in 0.1 to 10L containers. The samples for cation analysis and lead isotope analysis were pressure filtered through pre-weight teflon filters (SS). The filters were dried and equilibrated in an exsiccator before reweighing the filters. Two water blanks were transported into the field and treated like the other water samples.

The humic top layer was cut with a 0.3x0.3m frame. The top soil (0-5cm) and the mineral soil (5-40cm) samples were taken with a 7cm diameter corer. In the core sample the outer rim was peeled off to avoid downward contamination. The carbonate rocks were sampled (1997 and 1998) from outcrops in 5m diameter as unweathered carbonate chips in the total weight of 1-2kg.

Sample preparation for isotope analyses

5-10 L water samples were evaporated on a water bath or in a heating cabin (130°C) down to 0.5-0.3 L. 0.05-0.2 kg soil sample (105 °C dried and screened < 2mm; stored deep frozen) was leached with 0.8-1.2 L deionised water with continuous stirring over 24-34 hrs. The leachate was concentrated by heating (130°C) to 0.5-0.3 L. The BaSO₄ was precipitated after acidification (pH 3-4) with 2N HCl and adding 5-10 ml of 0.2N Ba Cl₂.2H₂O at moderate temperature (40-60 °C). The nitrogen, sulphur and oxygen isotopes of nitrate and sulphate were analysed by the labs of Univ. Lublin (Poland) and Hydroisotop Ltd (Munich, Germany).

Sr and Pb isotope analyses of water, soil and carbonate rock samples were performed in the Laboratory of Geochronology, University of Vienna and in the lab of the Environment Agency Vienna.

Results and discussion

To quantify and manage the problems resulting from the impact of air pollution on sensitive karst groundwater resources nitrogen-, sulphur- and lead-isotopes are used as key-indicators for a wide range of contaminants. Therefore they will be used for a new cost efficient control system, applied especially for surveillance of sensitive and remote areas.

In spite of strong efforts initiated by the European Union and other international organisations in the past 20 years, air pollution from industry, traffic and agriculture is still significant. Transboundary transport processes by atmospheric circulation are responsible for its long-range distribution. There is evidence that even remote mountainous regions in the Pyrenees or Alps as well as the Mediterranean islands are contaminated by inorganic and organic airborne pollution. This is most evident on the surface, but also penetrates into the aquifers, particularly in carbonate areas with strong karstification, characterised by dolines, karst shafts, caves and large springs. Special attention is therefore given in this project to karst aquifers: They are particularly vulnerable, but very important in many regions of Europe. Indeed, in many regions they are the only natural resources for drinking water supply.

In order to protect these water resources effectively the amount of the far transported pollutants should be identified and quantified at an early stage. For many transboundary pollution problems the time between recognition and relieve measures are in the range of ten years or more. In the last years, the monitoring was focused on surface water. However, airborne pollution of groundwater was rather neglected. To avoid the long term degradation of aquifer systems, new management tools and innovative alarm systems are urgently necessary. The UN-ECE-Integrated Monitoring station (Zoebelboden) is a background station with a very low sulphur (4-5 mg/l) and lead (0.2 µg/l) and a low nitrogen (5-7 mg/l) content in the karst water.

First results of this pilot investigation, which had to overcome the problem of extremely low concentrations will be shown in this presentation and further recommendation for the usage as surveillance tool will be given.

References

Kralik, M., HUMER, H., MIRTL, M., GRABNER, M., 2004. Hydrological and geo-chemical cycles in an alpine karst area: Austrian long term Integrated monitoring. Mountain Hydrology. In: HERRMAN, A. (ed.), Landschaftsökologie u. Umweltforsch. H. 47, 205-210, Braunschweig, Extended Abstr. Intern. Conf. on Hydrol. of Mountain Environments, 27. Sept.-1. Oct. 2004, Berchtesgaden.

Hydrological flow paths during snowmelt: Congruence between hydrometric measurements and oxygen18 meltwater, soil water and runoff

Hjalmar Laudon¹, Jan Seibert²
Stephan Köhler³, Kevin Bishop²

¹Department of Forest Ecology, Swedish University of Agriculture
Sweden, e-mail: hjalmar.laudon@emg.umu.se

²Department of Environmental Assessment, Swedish University of Agriculture
Sweden, e-mail: bishop@ma.slu.se

³Department of Applied Geosciences, Graz University of Technology
Austria, e-mail: koehler@tugraz.at

Streamflow generation in boreal catchments remains poorly understood. This is especially true for snowmelt episodes, which are the dominant hydrological event in many seasonally snow covered regions. We examined the spatial and temporal aspects of flowpaths by linking detailed oxygen 18 observations of stream, melt, soil and groundwater with hydrometric measurements in a small catchment in northern Sweden during snowmelt period. The results demonstrate that soil horizons below 90cm were hardly affected by the approximately 200m of snowmelt water infiltrating into the soil during spring. The approximately sixty-fold increase in runoff, from 0.13mm d⁻¹ to 8mm d⁻¹, was generated by a 30-40cm rise of the groundwater level. The total runoff during the snowmelt period from late April to late May was 134mm, of which 75% was present water. Mass balance calculations based on hydrometric and isotopic data independently, both using upscaling of a hillslope transect to the entire 13ha catchment, provided similar results of both water storage changes and the amount of event water that was left in the catchment after the snowmelt. In general, groundwater levels and runoff were strongly correlated, but different functional relationships were observed for frozen and unfrozen soil conditions. Although runoff generation in the catchment generally could be explained by the transmissivity feedback concept, the results suggest that there is a temporal variability in the flow pathways during the spring controlled by soil frost during early snowmelt.

References: Laudon, H., Seibert, J., Köhler, S.J. and Bishop, K., 2004. Hydrological flow paths during snowmelt: Congruence between hydrometric measurements and oxygen18 meltwater, soil water and runoff. *Water Res. Res.* 40, WO3102.

Constraining sedimentation rates in the Cretaceous of the Eastern Alps by carbon isotope stratigraphy

Stephanie Neuhuber¹, Michael Wagneich¹, Christoph Spötl²

¹Department of Geodynamics and Sedimentology, Universität Wien

Althanstrasse 14, A-1090 Wien, Austria, e-mail: stephanie.neuhuber@univie.ac.at

² Institut für Geologie und Paläontologie, Leopold-Franzens-Universität Innsbruck, Innrain
52, 6020 Innsbruck, Austria

Introduction

The application of stable isotope stratigraphy has been widely used in marine Cretaceous sediments. This technique uses temporally well-defined carbon isotope excursions as chemostratigraphic markers. Our poster presents the first application of stable isotope stratigraphy to Upper Cretaceous carbonates in the Eastern Alps. The studied section (Buchberg) was correlated to the absolutely dated chalk composite curve of Jarvis et al. (2006). The duration of so-called oceanic red beds in our section was constrained by correlating carbon isotope excursions to the chalk composite curve.

Methods

The stable carbon and oxygen isotope composition of bulk samples (micrite) was determined using a ThermoFinnigan DeltaPulsXL mass spectrometer equipped with a GasBench II following the procedure described in Spötl and Vennemann (2003). Trace element data (Mn/Sr vs. $\delta^{13}\text{C}$) were used to assess the degree of diagenesis (Jacobson and Kauffmann, 1999).

Sedimentation rates were calculated by comparison with the composite curve of Jarvis et al. (2006). Linear age-depth correlations were calculated using AnalySeries 2.0 (Paillard et al., 1996).

Results

Stable isotope data and trace element distribution suggest negligible diagenetic alteration. Biostratigraphy employing nannofossils and foraminifera (Perch-Nielsen, 1985) places the studied profile into the Lower to Middle Turonian. The main part of the profile was

deposited during the total range zone of *H. helvetica*. Within this zone several carbon isotope events were identified thus providing a higher temporal resolution.

The isotope events were calibrated based on the absolute timescale of Jarvis et al. (2006). The sedimentation rate in our section varies between 1 and 7 mm/kyrs. This further constrains the duration of oceanic red bed deposition to between 30 and 360 kyrs, whereas periods of grey marl deposition lasted between 70 and 470 kyrs.

References

- Jacobsen, S.B., Kaufman, A.J., 1999. The Sr, C and O isotopic evolution of Neoproterozoic seawater. *Chemical Geology* 161, 37-57.
- Jarvis, I., Gale, A.S., Jekyns, H.C., Pearce, M., 2006. Secular variation in Late Cretaceous carbon isotopes: a new $\delta^{13}\text{C}$ carbonate reference curve for the Cenomanian - Campanian (99.6-70.6 Ma). *Geological Magazine*, 143, 561-608.
- Paillard, D., Labeyrie, L., Yiou, P., 1996. Macintosh program performs time series analysis. *Eos, AGU* 77, 379.
- Perch-Nielsen, K., 1985. Mesozoic Calcareous Nannofossils. in: Bolli, H.M., Saunders, J.B., Perch-Nielsen, K. (Eds.) *Plankton Stratigraphy*. Cambridge University Press, Cambridge, pp 329-426.
- Spötl, C., Vennemann, T., 2003. Continuous -flow isotope ratio mass spectrometric analysis of carbonate minerals. *Rapid Communications in Mass Spectrometry*, 17, 1004-1006.

Application of $\delta^{18}\text{O}$ water analysis in the study of hydrological renewal in some Alpine Lakes

M. Perini, F. Camin, G. Flaim, F. Corradini, A. Tonon, G. Versini

Centro Sperimentale, Istituto Agrario di San Michele all'Adige, via Mach 1, 38010 San Michele all'Adige (TN) - Italy

$\delta^{18}\text{O}$ water analysis of five lakes (Lavarone, Caldonazzo, Levico, Serraiia and Tovel) located in Trentino (N Italy) was performed to better understand the dynamics and the modalities of hydrological renewal of the lakes in connection to seasonal mixing and thermal stratification of the water masses. The lakes considered have different hydrological regimes and their theoretical water renewal time varied from $> 1\text{ yr} - \geq 3\text{ yr}$.

Water samples were taken over the deepest part of the lake at discrete depths at least every 2 months and sometime the main tributaries (surface and underground) were sampled. Each lake was followed up for at least two years. Considerations on lake water renewal and on the stability of the hypolimnion and epilimnion for the different lakes are presented. The $\delta^{18}\text{O}$ values are fairly stable along the depth profile over the year for Tovel lake, whereas for the other lakes seasonal differences in $\delta^{18}\text{O}$ particularly in the epilimnion resulted. Different ^{18}O enrichments of epilimnion are shown for 2003 and 2004, due to the different climatic conditions of the two years.

The use of isotope measurements for the separation of discharge components at a karst spring during hydrological events

Dieter Rank¹, Wolfgang Papesch², Florian Wieselthaler¹

¹Center of Earth Sciences, University of Vienna, 1090-Vienna, Austria, e-mail: dieter.rank@univie.ac.at, ²ARC Seibersdorf research, 2444-Seibersdorf, Austria, e-mail: wolfgang.papesch@arcs.ac.at

The catchment area of the Wasseralmquelle (802 m.a.s.l.) is situated in the NE part of the Schneecalpe karst massif some 100 km SW of Vienna, in the northern “Kalkalpen”. Calculations from long-term isotope records from the Wasseralmquelle showed that reservoir water of this karst system has a mean residence time of about 26 years, while the short-term component has a transit time of 1,2 months (including retention time in the snow cover) (Maloszewski et al., 2002). For these calculations, the karstic reservoir is approximated by two different parallel flow systems, which provide water from the surface to the karstic springs. The first flow system, with a high storage capacity, consists mainly of mobile water in the fissures and quasi-immobile water in the porous matrix. The water enters this system through the whole surface of the catchment area and is collected into the drainage channels connected with the karstic springs. The drainage channels separately create a second flow system with a high velocity and small groundwater volume (very short mean transit time of water). This system is connected with sinkholes, which introduce precipitation water directly into this system. As a result, in the karstic springs there is a mixture of two water components: (1) flowing from the surface through fissured/porous medium to the drainage channels and then to the springs; and (2) flowing directly from the sinkholes through the drainage channels to the springs. The conceptual model of the water flow in the karstic catchment area of the Wasseralmquelle is shown in Fig. 1. This special form of the model for the Wasseralmquelle system includes also some infiltration of water from the channel system into the fissured-porous aquifer, since low precipitation depths (< 20 mm) do not lead to any increase of the discharge at the spring (Steinkellner 1997). In this case all precipitation water is infiltrating into the fissured-porous matrix.

Here we present some preliminary results of the Wasseralmquelle study in spring and summer 2005. Snow-melting periods with daily variations in discharge and heavy rainfalls in summer were selected for event investigations (Wieselthaler, 2006). Sampling with time resolution of one or two hours was provided at the Wasseralmquelle. Snow samples and rain samples, respectively, were collected for the determination of the input data.

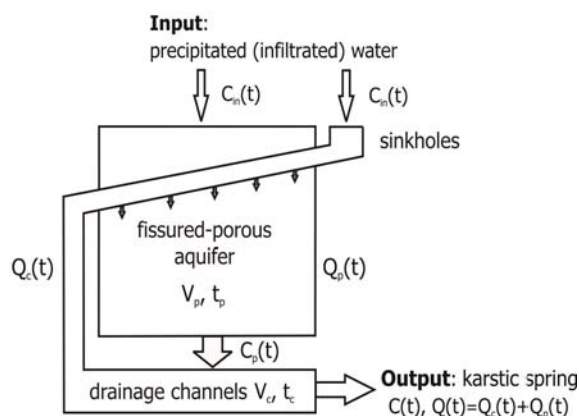


Figure 1. Conceptual model of water flow in the karstic system of the “Wasseralmquelle” (spring), modified after Maloszewski et al. (2002).

An example for the snow-melting investigations is shown in Fig. 2. Air temperature maxima, causing snow melting on the plateau of Schneealpe during the day, lead to an increase in discharge at the spring and a decrease in electrical conductivity (EC) in spring water, with a delay of approximately 16 hours (daily variations). The graph of the $\delta^{18}\text{O}$ -values develops similarly like the graph of electrical conductivity and indicates times of higher melting-water content in the discharge. At the end of the sampling period, air temperature drops, melting-water content decreases and therefore $\delta^{18}\text{O}$ -values and electrical conductivity are rising again.

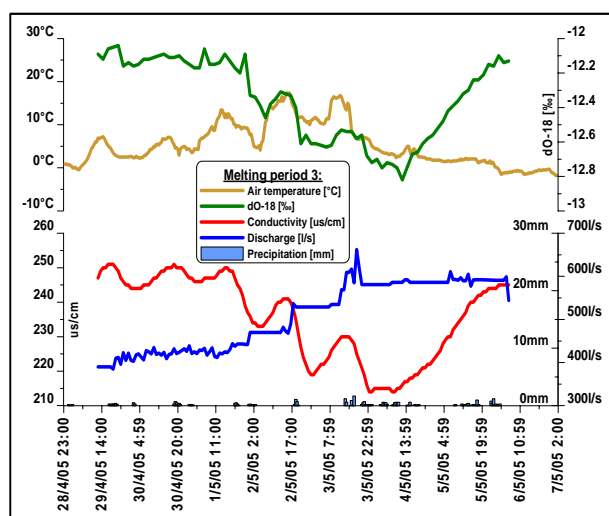


Figure 2. Example for the course of discharge, electrical conductivity and $\delta^{18}\text{O}$ in springwater of the Wasseralmquelle, air temperature and amount of precipitation on the plateau of the karst massif during a typical snow-melting period with daily variations (28.04.05 – 07.05.05) (Wieselthaler, 2006).

The investigations of rain events in summer - when we can expect the most significant ^{18}O signals – give information about the direct precipitation/discharge relation. An example for such an investigation is shown in Fig. 3 and Fig. 4. Heavy rainfalls during July 7 and 8 lead to an increase of the discharge from 300 l/s up to 800 l/s (Fig. 3). ^{18}O -content and EC changes at the same time show that event water contributes from the beginning to the increase of the discharge. The separation of discharge components yielded a content of up to 50 % of event water in the discharge of the Wasseralmquelle during the discharge peak (Fig. 4). After the discharge peak the amount of base flow remains increased. The karst-water level in the matrix is obviously raised by infiltrated event water and this leads to a larger base flow component. The results of the separation calculation indicate that about 8 % of the total precipitation water from the drainage area had passed the spring three days after the precipitation event.

Conclusions

The discharge of the Wasseralmquelle during hydrological events shows a clear two-component case. Although the baseflow water has a mean residence time of 26 years (calculated from ^3H records), event water (precipitation, snow melting) appears in the spring after a few hours with the first increase of the discharge. Most of the additional discharge at the beginning consists of event water. This water reaches the spring through “quick” channels in the karst system.

Regarding isotope ratios, EC and temperature, the spring waters from the different outlets in the spring galleries show the same origin. This is evidence for a bigger, well mixed karst reservoir, at least in the vicinity of the spring and during base flow conditions.

In the case of the Wasseralmquelle it turns out that EC of the springwater is probably not a suitable parameter for the separation of short-term discharge components. The electrical conductivity of the infiltrating precipitation water increases relatively quickly in the karstic system.

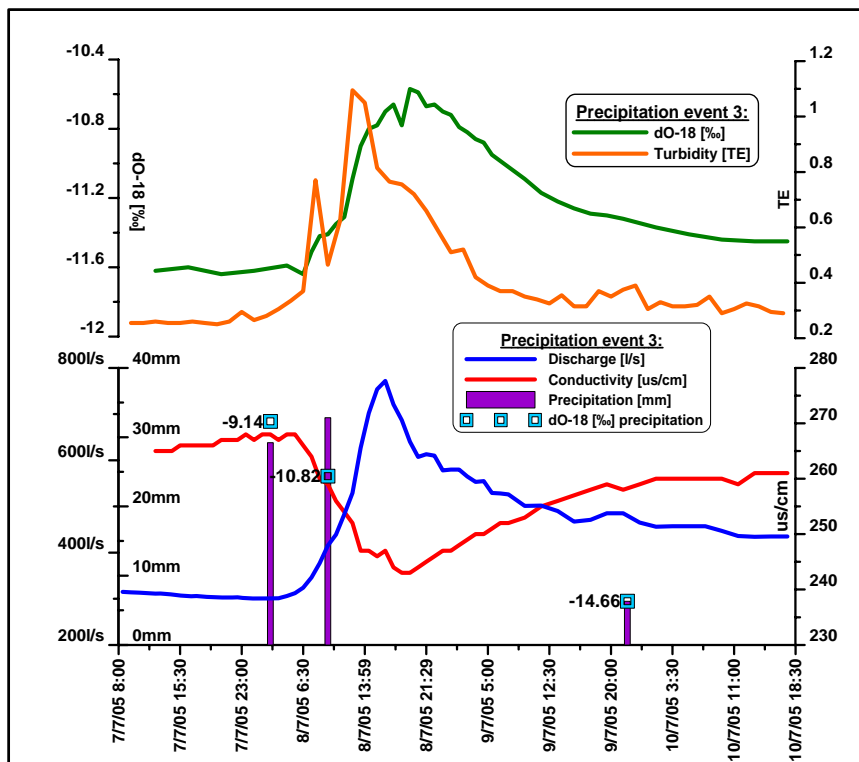


Figure 3. Example for the course of discharge, electrical conductivity, turbidity and $\delta^{18}\text{O}$ variations in springwater of the Wasseralmquelle during a strong precipitation event, amount of precipitation and $\delta^{18}\text{O}$ -values of the rainwater samples from the plateau of the karst massif (07.07.05 – 10.07.05).

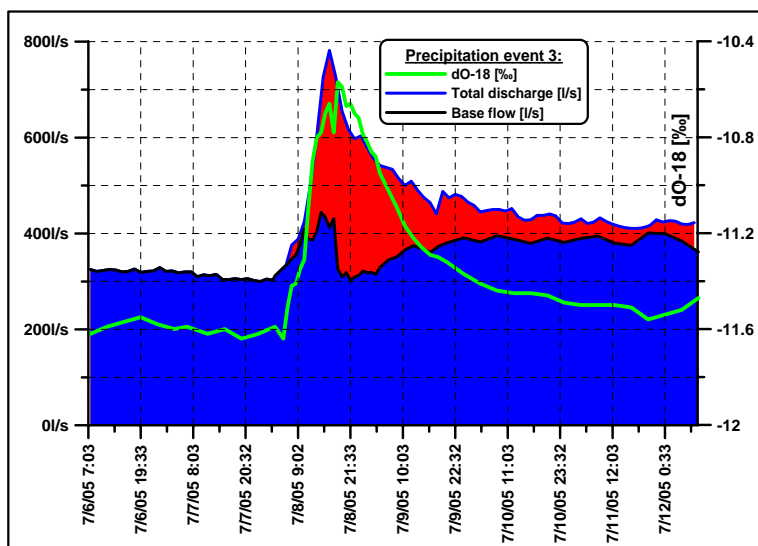


Figure 4. Separation of discharge components for precipitation event 3 (see Fig.3).

References

- Maloszewski, P., Stichler, W., Rank, D., Zuber, A., 2002. Identifying the flow systems in a karstic-fissured-porous aquifer, the Schneealpe, Austria, by modelling of environmental ^{18}O and ^3H isotopes. *Journal of Hydrology* 256, 48-59.
- Steinkellner, M., 1997. Auswertung der Ganglinien der Wasseralmquelle 1, Studie im Auftrag der Wiener Wasserwerke (MA 31 07/3853/760), TBMS-97/03, St. Lorenzen.
- Wieselthaler, F., 2006. Abflusskomponentenanalyse bei einer Karstquelle auf der Basis von Ereignisuntersuchungen, diploma thesis, Univ. of Vienna, Vienna, 110 pp.

Stable isotope production in Russia

Mudis Šalkauskas

Lithuanian Society of Chemists,

A. Goštauto 9, LT-01108 Vilnius, Lithuania, e-mail: mudis@ktl.mii.lt

In Russia there are great numbers of well-equipped laboratories and semi plants that may produce many stable isotopes of high purity and in great quantities. As far as they use various efficient equipments the price of isotopes is comparatively low. As far as the Russia is not yet a member of WTO or EU, sometimes there are problems in supply. Therefore some sub suppliers from new EU countries may help to solve them in a short time. One of such is Lithuanian Joint Stock Co. "ISOTOPUS".

References

www.gamma-lab.com

www.c13.ru

www.ecp.kts.ru

Experimental Crystallization of CaCO₃ Polymorphs for Sr²⁺/Ca²⁺ and ⁴⁴Ca/⁴⁰Ca Fractionation

Jianwu Tang¹, Stephan Köhler¹, Martin Dietzel¹, Albrecht Leis²

¹Institute of Applied Geosciences, Graz University of Technology, Rechbauerstrasse 12,
8010 Graz, Austria

²Institute of Hydrogeology and Geothermics, Elisabethstrasse 16/11,
8010 Graz, Austria

Trace elements and isotopes fractionate during CaCO₃ crystallization. The degree of fractionation is commonly influenced by CaCO₃ crystallization environments and may be used as a proxy to reconstruct paleoenvironments (such as T and solution chemistry). In this study, CO₂ Diffusion Technique (CDT; e.g. Dietzel et al., 2004) and Double Diffusion Technique (DDT; e.g. Prieto et al., 1997) are used to crystallize CaCO₃ polymorphs. The aim is to assess the impact of temperature, precipitation rate, solution chemistry, cation diffusion, and CaCO₃ polymorphs on Sr²⁺/Ca²⁺ and calcium isotope fractionation in inorganic systems.

The experimental results indicate that at a temperature range from 5° to 40°C, single type of CaCO₃ polymorphs (calcite and aragonite) can be produced by controlling the aqueous Mg²⁺/Ca²⁺ molar ratio and the precipitation rate, R_{calcite} ($\mu\text{mol m}^{-2} \text{h}^{-1}$), in the reaction solution. For example, for CDT a Mg²⁺/Ca²⁺ molar ratio less than 0.01 yields calcite as sole precipitate, whereas a ratio of about 2 exclusively induces aragonite formation. Most calcite crystals exhibit rhombohedral habit. Aragonite occurs as fibrous crystals, usually in radiating groups.

The Sr²⁺/Ca²⁺ distribution between aqueous solution and CaCO₃ minerals is very sensitive to polymorphs due to the respective crystal type. Under all experimental conditions, Sr²⁺/Ca²⁺ molar ratios in aragonite are higher than that in calcite at analogous experimental conditions. Accordingly, e.g. for calcite a continuous enrichment of aqueous Sr²⁺ vs. Ca²⁺ in reaction solution is observed, caused by Sr²⁺ discrimination in the crystal lattice, which can be followed by a Rayleigh fractionation process.

The results show that the distribution coefficient of Sr²⁺ into calcite, $D_{\text{Sr}} = (\text{Sr}^{2+}/\text{Ca}^{2+})_{\text{calcite}} / (\text{Sr}^{2+}/\text{Ca}^{2+})_{\text{aq}}$ is positively correlated to the precipitation rate (R_{calcite}) at a constant temperature of 5°, 25°, and 40°C. Elevated precipitation rates usually lead to lower

discrimination effects during the precipitation (see also Lorens, 1981; Tresorio and Pankow, 1996).

However, the value of D_{Sr} for calcite is also influenced by temperature. At an identical precipitation rate D_{Sr} values show a negative temperature dependence (also Dickson, 1985 and Rimstidt et al., 1998). In general, slopes for $\log(D_{Sr})$ vs. $\log(R)$ decrease from high temperature to low temperature, which indicates that precipitation rate effect is enlarged at lower temperatures. At very low precipitation rates the overall temperature effect might be small. In this case, Sr discrimination in calcite may be controlled by slow precipitation kinetics or even by equilibrium fractionation. Further experiments at low precipitation rates have to be carried out by using CDT with seed crystals to verify this behavior.

Up to now, distribution of $^{44/40}Ca$ are analyzed for several experiments at 40°C at elevated precipitation rates. Our data lay between the results for stirred and unstirred experiments for spontaneous calcite growth at 21°C from Lemarchand et al. (2004). Thus, preliminary results indicate that temperature may have a minor impact on $^{44/40}Ca$ isotope fractionation during calcite precipitation.

Experiments using DDT show that cation diffusion in gel follows the order of $Ba > Ca > Sr > Mg$ and ^{40}Ca diffuses faster than ^{44}Ca at 25°C. The degree of fractionation may be caused by individual diffusion coefficients and the structure of the gel. In terms of the overall Ca isotope fractionation by calcite crystallization, diffusion effect is highly significant. Measured overall Ca isotope fractionation for calcite, $\Delta^{44/40}Ca_{calcite-Ca^{2+}}$, from DDT is for example about -1 ‰, whereas $\Delta^{44/40}Ca_{Ca^{2+} \text{ diffusion}}$ due to calcium diffusion without $CaCO_3$ formation ranges from -0.4‰ to -1.5‰, depending on the diffusion length and concentration gradient.

References

- Dickson, J.A.D., 1985. Sedimentology – Recent Developments and Applied Aspects, 173-188.
- Dietzel, M., Gussone, N., Eisenhauer, A., 2004. Co-precipitation of Sr^{2+} and Ba^{2+} with aragonite by membrane diffusion of CO_2 between 10 and 50°C. Chemical Geology 203, 139-151.
- Lemarchand, D., Wasserburg, G.J., Papanastassion, D.A., 2004. Rate-controlled calcium isotope fractionation in synthetic calcite. Geochim. Cosmochim Acta 68, 4665-4678.

- Lorens, R.B., 1981. Sr, Cd, Mn and Co distribution coefficients in calcite as a function of calcite precipitation rate. *Geochim. Cosmochim. Acta* 45, 553-561.
- Prieto, M., Fernández-González, A., Putnis, A., Fernández-Díaz, L., 1997. Nucleation, growth, and zoning phenomena in crystallizing (Ba,Sr)CO₃, Ba(SO₄,CrO₄), (Ba,Sr)SO₄, and (Cd,Ca)CO₃ solid solutions from aqueous solutions. *Geochim. Cosmochim. Acta* 61, 3383-3397.
- Rimstidt, J.D., Balog, A., Webb, J., 1998. Distribution of trace elements between carbonate minerals and aqueous solutions. *Geochim. Cosmochim. Acta* 62, 1851-1863.
- Tesoriero, A., Pankow, J.F., 1996. Solid solution partitioning of Sr²⁺, Ba²⁺, and Cd²⁺ to calcite. *Geochim. Cosmochim. Acta* 60, 1053-1063.

Comparison of monthly and daily isotopic composition of precipitation in south-western Slovenia

Polona Vreča¹, Albrecht Leis², Zdenka Trkov¹, Stojan Žigon¹, Sabine Lindbichler²

¹ "Jožef Stefan" Institute, Department of Environmental Sciences,
Jamova 39, SI-1000 Ljubljana, Slovenia, e-mail: polona.vreca@ijs.si

² Joanneum Research, Institute of Water Resources Management (WRM), Elisabethstrasse
16/II, A-8010 Graz, Austria

Introduction

Precipitation is of major interest in the hydrologic cycle as it is the ultimate source of water to catchments. The terrestrial portion of the hydrologic cycle begins when the precipitation reaches the ground. Therefore, the understanding of the formation of precipitation, as well as knowledge of temporal and spatial variations in the amount and mode of precipitation are important for basin-wide balance studies. Similarly, understanding how isotopic composition ($\delta^{18}\text{O}$ and $\delta^2\text{H}$) is controlled by the formation of precipitation and knowledge of the temporal and spatial variations in isotopic composition of precipitation are equally important. Within the Global Network of Isotopes in Precipitation (GNIP) organised by IAEA and WMO worldwide monitoring of isotopes in precipitation is performed. The GNIP database is thus extremely valuable for modelling of climatic changes as well as in hydrological and hydrogeological investigations.

Monitoring of isotopes in monthly precipitation has been performed at continental sampling station in Ljubljana (Slovenia) since 1981 within the GNIP (Vreča et al., 2006). In the framework of IAEA Co-ordinated Research Program "Isotopic Composition of Precipitation in the Mediterranean Basin in Relation to Air Circulation Patterns and Climate" the monitoring program was extended to two additional sampling stations in south-western, Mediterranean region of Slovenia in October 2000 (Vreča et al., 2005). In this study, we present 1-year long monthly, as well as daily records of isotopic composition in precipitation together with meteorological data from two stations in Slovenian Mediterranean region.

Sampling and analyses

Samples were collected from October 2002 till September 2003 at coastal station Portorož Airport (45°28'N, 13°37'E) and at station close to the coast in Kozina (45°36'N, 13°56'E). Monthly composite precipitation sample was collected in a rain gauge with diameter of 16 cm. Daily samples were collected in the morning after precipitation event in a rain gauge with a diameter of 54 cm. Meteorological data (precipitation amount and temperature) were obtained from the Environmental Agency of Republic of Slovenia for station at Portorož Airport, while for Kozina only data on precipitation amount were available.

The stable isotopic composition of water samples was measured on a dual inlet Varian MAT 250 mass spectrometer at the Jožef Stefan Institute and on a continuous flow Finnigan DELTA^{plus} XP mass spectrometer with a HEKAtech high-temperature oven at Institute of Institute of Water Resources Management (WRM). The oxygen isotopic composition ($\delta^{18}\text{O}$) was measured by means of the water-CO₂ equilibration technique, and the isotopic composition of hydrogen ($\delta^2\text{H}$) was performed using H₂ generated by reduction of water over hot chromium. Measurement reproducibility of duplicates was better than $\pm 0.05\text{‰}$ for $\delta^{18}\text{O}$ and $\pm 1\text{‰}$ for $\delta^2\text{H}$.

Results and discussion

Stable isotopic composition of precipitation varies considerably at both sampling stations. In monthly collected samples $\delta^{18}\text{O}$ values vary between -10.6 and -1.6‰ (mean -5.7‰) at Portorož Airport, and between -13.8 and -3.6‰ (mean -7.7‰) in Kozina. $\delta^2\text{H}$ values vary between -80 and -8‰ (mean -36‰) at Portorož Airport, and between -102 and -23‰ (mean -50‰) in Kozina. The highest values are observed at the coastal station at Portorož Airport and lower, due to continental and altitude effect, at Kozina. Obtained data fit very well to the Craig's Global Meteoric Water Line (GMWL) however some deviations were observed in summer months at Portorož Airport and are probably a result of partial evaporation of raindrops (Table 1). *d-excess* values vary between 3 and 19‰ (mean 10‰) at Portorož Airport, and between 4 and 18‰ (mean 12‰) in Kozina. The lowest values were observed during May and August, respectively. The comparison of obtained stable isotopic data with precipitation amount showed no significant correlation. In contrast, significant correlation between stable isotopic data and air temperature was observed at Portorož Airport.

Table 1. Local meteoric water lines for Portorož Airport and Kozina.

Portorož Airport (monthly)	$\delta^2\text{H} = 7.4 \delta^{18}\text{O} + 6.2$	r= 0.97
Portorož Airport (daily)	$\delta^2\text{H} = 6.7 \delta^{18}\text{O} - 0.6$	r= 0.95
Kozina (monthly)	$\delta^2\text{H} = 7.8 \delta^{18}\text{O} + 10.0$	r= 0.98
Kozina (daily)	$\delta^2\text{H} = 7.8 \delta^{18}\text{O} + 7.9$	r= 0.98

Considerable daily variations in stable isotopic composition were observed during observation period. $\delta^{18}\text{O}$ values vary between -14.9 and $+3.5\text{‰}$ (mean -4.5‰) at Portorož Airport, and between -17.5 and $+1.2\text{‰}$ (mean -7.1‰) in Kozina. $\delta^2\text{H}$ values vary between -112 and $+8\text{‰}$ (mean -31‰) at Portorož Airport, and between -134 and $+3\text{‰}$ (mean -47‰) in Kozina. *d-excess* values vary between -20 and 27‰ (mean 5‰) at Portorož Airport, and between -16 and 26‰ (mean 10‰) in Kozina. Higher values were observed at the start of precipitation event and decreased during precipitation event. Obtained data fit well to the GMWL at Kozina while at Portorož Airport the influence of evaporation during extremely warm period (spring-summer 2003) is reflected in data below the GMWL (Table 1).

Furthermore, mean monthly amount-weighted isotopic composition was calculated from individual daily data and compared to results obtained for individual monthly samples (Table 2). The differences between both set of results could be attributed to:

- 1) difference in precipitation amount of monthly sample and daily collected samples (e.g. not all daily samples were collected in December 2002, January, March and April 2003);
- 2) position of sampling rain gauges (approx. 10-20 m apart);
- 3) different diameter of sampling rain gauges;
- 4) evaporation effect during extremely warm and dry year 2003 (e.g. July 2003 at Portorož Airport).

Table 2. Comparison of isotopic composition of monthly collected samples (m) and monthly isotopic composition calculated amount-weighted isotopic composition from individual daily data (wdm) at Portorož Airport and Kozina.

Month/ Year	Portorož Airport				Kozina			
	$\delta^2\text{H}_m$ (‰)	$\delta^2\text{H}_{wdm}$ (‰)	$\delta^{18}\text{O}_m$ (‰)	$\delta^{18}\text{O}_{wdm}$ (‰)	$\delta^2\text{H}_m$ (‰)	$\delta^2\text{H}_{wdm}$ (‰)	$\delta^{18}\text{O}_m$ (‰)	$\delta^{18}\text{O}_{wdm}$ (‰)

10/2002	-24	-30	-5.3	-5.8	-47	-47	-8.0	-7.8
11/2002	-25	-35	-5.3	-5.6	-45	-44	-7.3	-7.4
12/2002	-58	-36	-9.1	-5.7	-77	-86	-11.4	-12.2
1/2003	-68	-54	-10.2	-7.2	-102	-91	-13.8	-12.3
2/2003	-80	-76	-10.6	-10.9	-80	-77	-11.3	-11.4
3/2003	-17	-16	-3.2	-3.8	-23	-50	-5.2	-7.7
4/2003	-46	-39	-6.6	-4.8	-66	-68	-9.7	-9.5
5/2003	-20	-20	-3.0	-2.7	-34	-34	-5.8	-5.4
6/2003	-31	-32	-4.5	-4.3	-31	-33	-5.0	-4.9
7/2003	-8	-6	-1.6	-0.9	-25	-23	-3.8	-3.0
8/2003	-21	-21	-3.2	-2.8	-25	-20	-3.6	-2.1
9/2003	-30	-37	-5.6	-6.0	-45	-51	-7.8	-7.7

Conclusion

Comparison of monthly and daily isotopic composition of precipitation showed differences between both set of data and indicates the need for short-term determination of isotopic composition that would enable better understanding of the effect of changing meteorological conditions that are lost during long-term (e.g. monthly) collection of precipitation samples.

References

- Vreča, P., Krajcar Bronić, I., Horvatinčić, N., Barešić, J., 2006. Isotopic characteristics of precipitation in Slovenia and Croatia: comparison of continental and maritime stations. *Journal of Hydrology* 330, 457-469.
- Vreča, P., Kanduč, T., Žigon, S., Trkov, Z., 2005. Isotopic composition of precipitation in Slovenia. In: *Isotopic composition of precipitation in the Mediterranean basin in relation to air circulation patterns and climate: final report of a coordinated research project 2000-2004*, (IAEA-TECDOC, 1453). Vienna: IAEA, 157-172.

Analysis of carbon isotope composition of plant carbohydrates

Wolfgang Wanek, Andreas Richter

Department of Chemical Ecology and Ecosystem Research, University of Vienna
Althanstrasse 14, A-1090 Wien, Austria

Starch is the main carbon storage carbohydrate in plants. It is considered as one of the most abundant organic compound on earth, second only to other carbohydrates such as cellulose. The carbon isotope composition of starch has been studied with regard to different photosynthetic pathways and the water-use efficiency of plants mainly in the 1970s and 80s. Recently, the carbon isotope composition of plant carbohydrates has attracted renewed interest, since these compounds are thought to be major substrates of autotrophic respiration. Therefore, the knowledge of the isotopic signature of these compounds is a prerequisite to determine the contribution of heterotrophic respiration to the terrestrial carbon flux.

At present, several methods for the isolation and determination of carbon isotope composition of starch are available. However, a comparison of these methods has shown that the methods yield very different results for both amount and carbon isotope composition. We here report on an inter-laboratory comparison aiming (1) comparing the available methods on both an "artificial" plant material (a mixture of isotopically defined, commercially available plant constituents) and a range of different plant tissues, (2) identifying possible sources of errors for the different methods and (3) recommending a reference method to enhance the comparability of isotope data in this field.

All methods for starch determination, and for isolation of starch from plant material for isotopic measurements, is based on a three step procedure: the removal of soluble sugars by excessive washing with aqueous media, the hydrolysis of starch by acid or enzymatic means, and the purification of the hydrolysate by precipitation of hydrolyzed starch (acid hydrolysis) or removal of enzyme by dialysis or ultrafiltration (enzymatic hydrolysis).

Both approaches, i.e. acids and enzymatic hydrolysis, are prone to several (potential) problems. First, suitable reference materials and reference methods for quantification, and particularly for isotope composition in starch, are lacking. Second, incomplete removal of soluble sugars and other low-molecular weight compounds prior to starch hydrolysis can contaminate of the starch hydrolysates. Third, the methods should selectively hydrolyze starch but leave other high-molecular weight compounds unchanged. Contamination can derive from hydrolysable organic carbon compounds such as hemicelluloses, cellulose, gums

(mucilages, pectins) and condensed polyphenols but also from proteins. Fourth, complete hydrolysis of starch has to be ensured since starch granules may be isotopically inhomogeneous.

From the experiments we conclude:

- (1) the methods based on acid hydrolysis and on enzymatic hydrolysis of starch are not comparable with regard to carbon isotope composition and content.
- (2) The specificity (selectivity) of the methods based on the acidic hydrolysis was low, and we therefore suggest terming these preparations as HCl-hydrolysable carbon, rather than starch.
- (3) The methods based on enzymatic hydrolysis at the moment provide the only feasible way for a compound-specific analysis of isotopes in starch.

Index of names

BALAS, G.	11	NEUHUBER, S.	30
BAUMGARTEN, M.	22	NURMI-LEGAT, J.	25
BISHOP, K.	29		
BOJAR, A.-V.	3	OTTNER, F.	3
BOJAR, H.-P.	3		
		PALIBRODA, N.	11
CAMIN, F.	33	PAPESCH, W.	34
CORRADINI, A.	33	PENDALL, E.	6
CUNA, S.	6, 11	PERINI, F.	33
DIETZEL, M.	13, 22, 40	RANK, D.	34
DLUGOKENCKY, E.	6	REICHL, P.	13
		RICHTER, A.	47
FLAIM, G.	33	RINDER, T.	13
GRIGORESCU, D.	3	SALKAUSKAS, M.	39
GRABNER, M.-T.	25	SEIBERT, J.	
GRATH, J.	25	SPÖTL, C.	30
GUSSONE, N.	19	STINGL, K.	22
HALAS, S.	25	TANG, J.	40
HANUS-ILNAR, A.	25	TANS, P.P.	6
HUMER, F.	25	TONON, A.	33
		TRKOV, Z.	43
JELENC, M.	25		
		VERSINI, G.	33
KOSEDNAR-LEGENSTEIN, B.	22	VRECA, P.	43
KLAMMER, D.	13		
KÖHLER, S.	13, 29, 40	WAGREICH, M.	30
KRALIK, M.	25	WANEK, W.	47
		WIEGAND, B.	22
LAUDON, H.	29	WIESELTHALER, F.	34
LEIS, A.	13, 22, 40, 43		
LINDBICHLER, S.	43	ZIGON, S.	43
MILLER, J.B.	6		
MIRTL, M.	25		

Sponsors

